THE JOURNAL OF THE ACOUSTICAL SOCIETY OF KOREA Vol.21, No.4E 2002. 12. pp. 183~188

# Observation of Strong In-plane End Vibration of a Cylindrical Shell

Hyun-Gwon Kil*
*Department of Mechanical Engineering, University of Suwon
(Received 6 November 2002; accepted 13 December 2002)

**Abstract**

In this paper, the strong in-plane vibration has been experimentally observed at the end of a finite cylindrical shell. The strong in-plane vibration was generated by the evanescent wave field, which was excited along about half the length of the shell. The evanescent waves were generated due to mode conversion of elastic waves at the ends of the cylindrical shells. The results show that the strong in-plane end vibration can be generated in cylindrical shells.

***Keywords:*** *End vibration, Cylindrical shell, Evanescent waves*

## I. Introduction

Vibration of a cylindrical shell is generated due to elastic waves propagating on the shells. Those elastic waves include propagating waves such as flexural, longitudinal and shear waves. Those also include non-propagating decaying waves, i.e. evanescent waves. The evanescent waves are generated near a force point and near ends of the cylindrical shell. Their contribution to vibration is generally confined to corresponding nearfields. But strong in-plane end vibration due to evanescent waves had been experimentally observed at ends of a cylindrical rod and disks[1,2]. The similar phenomena had been observed theoretically at an end of a semi-infinite plate[3] and recently at an end of a semi-cylindrical shell[4].

In this paper, the strong in-plane vibration has been experimentally observed at the end of a finite cylindrical shell. The strong in-plane vibration was generated by the evanescent wave field, which was excited along about half the length of the shell. The evanescent waves were generated due to mode conversion of elastic waves at the ends of the cylindrical shells. The results show that the strong in-plane end vibration can be generated in cylindrical shells.

Corresponding author: Hyun-Gwon Kil (hgkil@mail.suwon.ac.kr) Department of Mechanical Engineering, University of Suwon, San 2-2, Wau-ri, Bongdam-up, Whasung-shi, Kyunggi-do, 445-743, Korea

## II. Analysis of Experimental Data

### 2.1. Experiment

The experimental model is a finite cylindrical shell made of stainless steel. The dimensions of the shell are : $L=0.94\ m$, $a=0.076\ m$, $h=0.0015\ m$. In order to approximate the free-free boundary conditions at both ends of the shell, the shell was held between two aluminum end caps with four uniformly spaced pieces of materials such as neoprene and corprene along each end of the shell as shown in Fig. 1. The shell was excited by a piezoelectric shaker located inside of the shell and $0.32L$ above the bottom of the shell. The shaker was driven at a frequency $18275\,Hz$ corresponding to $1.65f_r$

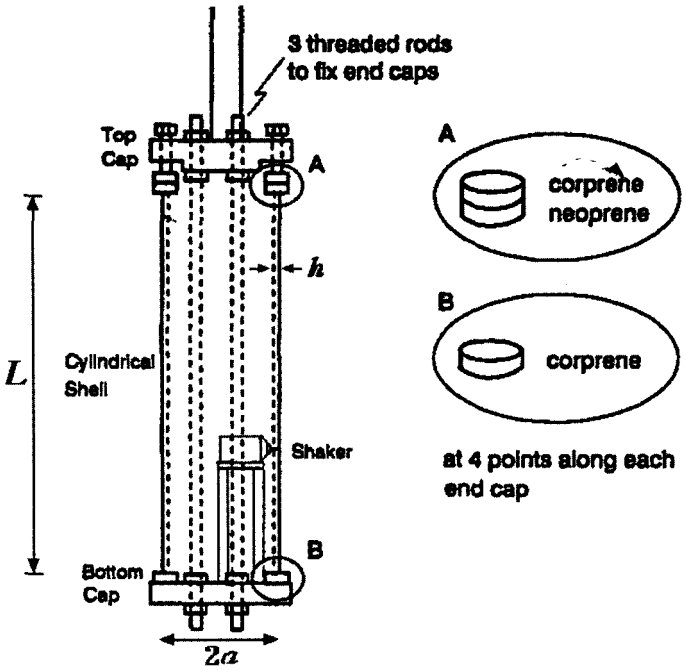


Figure 1. Experimental cylindrical shell with $L=0.94\ m$, $a=0.076\ m$ and $h=0.0015\ m$.

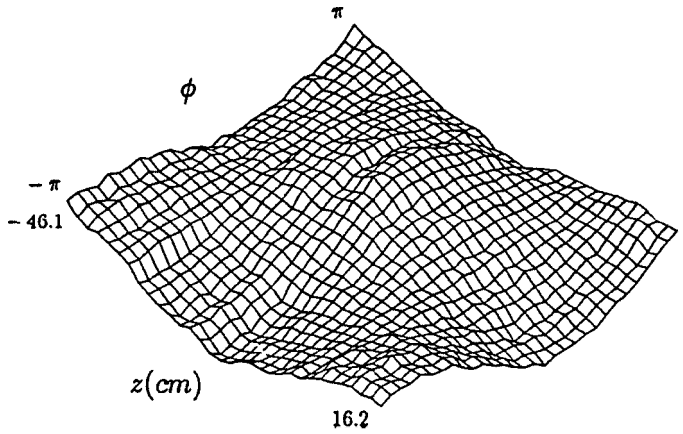


Figure 2. The axial displacement field $u(\phi,z)$ measured over the cylindrical shell at $18275\,Hz$.

where $f_r=11,059\ Hz$ is a ring frequency of the cylinder. The frequency was chosen considering the strong axial vibration at the end of the experimental shell. The laser Doppler vibrometry system was used to measure the in-plane vibration of the shell. The detailed description about the experimental system can be found in Ref.[5]. Two different wave fields are generated on the regions of the shell above and below the excitation point. The axial displacement was measured at $32\times32$ points on the surface of the shell above the excitation point.

## 2.2. Analysis of Experimental Data and Results

Consider the given circular frequency $\omega$ and the axial displacement $u(\phi,z)e^{-i\omega t}$ over the cylindrical shell described using the cylindrical coordinate ($r=a$, $\phi$, $z$). Fig. 2. shows the axial displacement field $u(\phi,z)$ measured over the cylindrical shell. It shows the regular modal patterns, especially $n=1$ circumferential mode along the circumference. However, it is difficult to separate the contributions of various waves, which are combined into the total displacement field. Those contributions of the waves can be separated by performing wave-vector analysis

based on the Fourier Transform. The axial displacement data $u(\phi,z)e^{-i\omega t}$ can be processed to evaluate the wave spectrum $U_n(k_z)$[6] at the frequency $\omega$ as

$$U_n(k_z)=\frac{1}{2\pi}\int_{-\infty}^{\infty}\int_0^{2\pi}u(\phi,z)e^{ik_z z}e^{in\phi}d\phi\,dz \qquad (1)$$

Here, $n(=k_\phi a)$ means to circumferential wavenumber index. $k_\phi$ and $k_z$ correspond to circumferential and axial wavenumbers, respectively. The wave spectrum $U_n(k_z)$ physically means the complex amplitude of wave propagating in the direction of the wavenumber vector

$$\tilde{k}=k_\phi\,\tilde{e}_\phi+k_z\,\tilde{e}_z \qquad (2)$$

where $\tilde{e}_\phi$ and $\tilde{e}_z$ mean the unit vectors in circumferential and axial directions, respectively.

The fast Fourier transform(FFT)[7] algorithm is well suited to perform the wave vector representation of Eq.(1). Fig. 3 shows the result of the wave spectrum $U_n(k_z)$ obtained with the FFT of the experimental data $u(\phi,z)$. Each peak on the wave spectrum is associated with the amplitude of a wave propagating in the direction defined by the corresponding wavenumber vector in Eq.(2). Strong peaks appear in the low wavenumber region while weak peaks appear in the high wavenumber region. The weak peaks correspond to flexural waves. The strong peaks are associated with the in-plane waves such as longitudinal

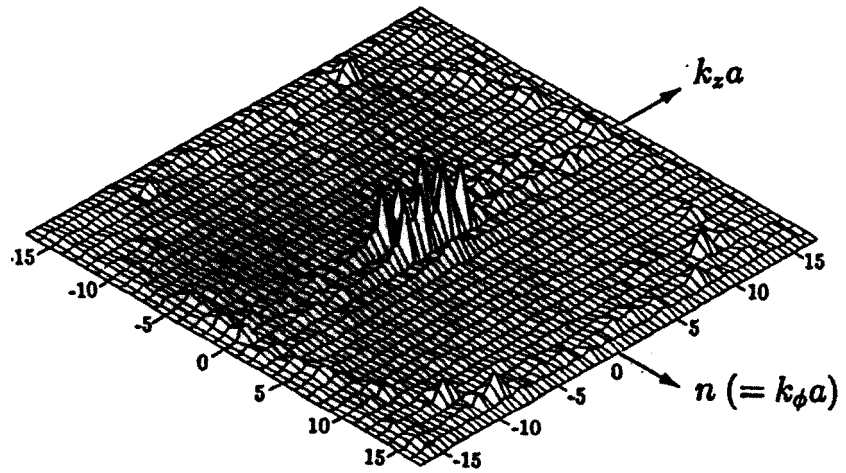


Figure 3. The wave spectrum $U_n(k_z)$ obtained with the FFT of the experimental data $u(\phi,z)$ at 18275 $Hz$.

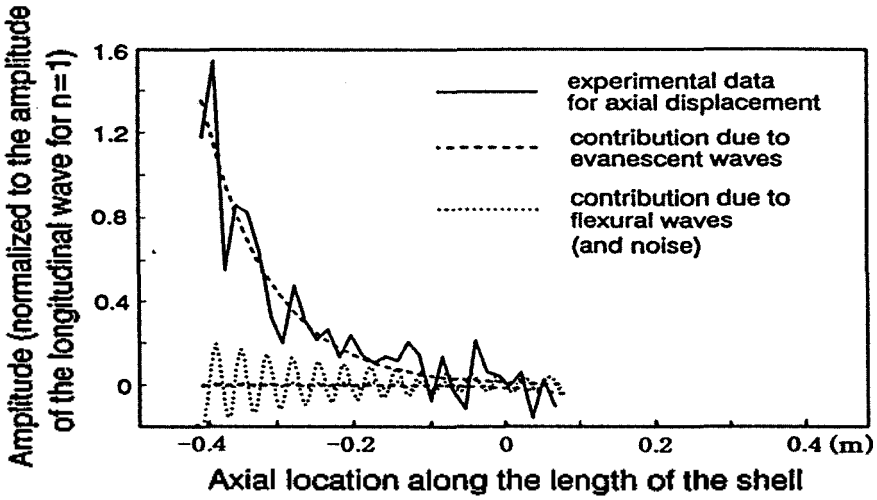


Figure 4. Decomposition of the experimental axial displacement data with the dependence of $n=3$, $u_3(z)$, by means of the Prony method to illustrate the presence of the evanescent wave.

and shear waves, which dominantly excite the in-plane vibration of the shell.

The wave spectrum in Fig. 3 shows the broad peak around $n=3$ and $k_z=0$ in the wavenumber plane. In order to investigate the characteristics of waves generating the broad peak, the displacement data with the dependence of $n=3$, $u_3(z)$, along the length of the shell is analyzed with the Prony method. The Prony method models the data with exponentials of arbitrary complex amplitudes (magnitudes and phases) and complex wave numbers (wave numbers and damping terms) which are found by a least-square minimization of the difference between the experimental data and the reconstructed data sets. It models the data as

$$u_3(z) = \sum_{m=1}^{M} [A_j^+ e^{-ik_{zm}} + A_j^- e^{ik_{zm}}] \tag{3}$$

Here $A_j^+$ and $A_j^-$ correspond to the amplitudes of waves propagating in directions of $+z$ and $-z$, respectively. $M$ means the total number of waves with the corresponding axial wave number and a given circumferential wave index $n$ at a given frequency. $M$ corresponds to 4 in the cylindrical shell. The detailed algorithm of the Prony method can be found in Ref.[8,9]. Fig. 4 shows the results obtained with the Prony method. The solid line represents the measured data. The dotted lines represent the contributions of flexural and evanescent waves into the measured data. The result clearly reveals the presence of an

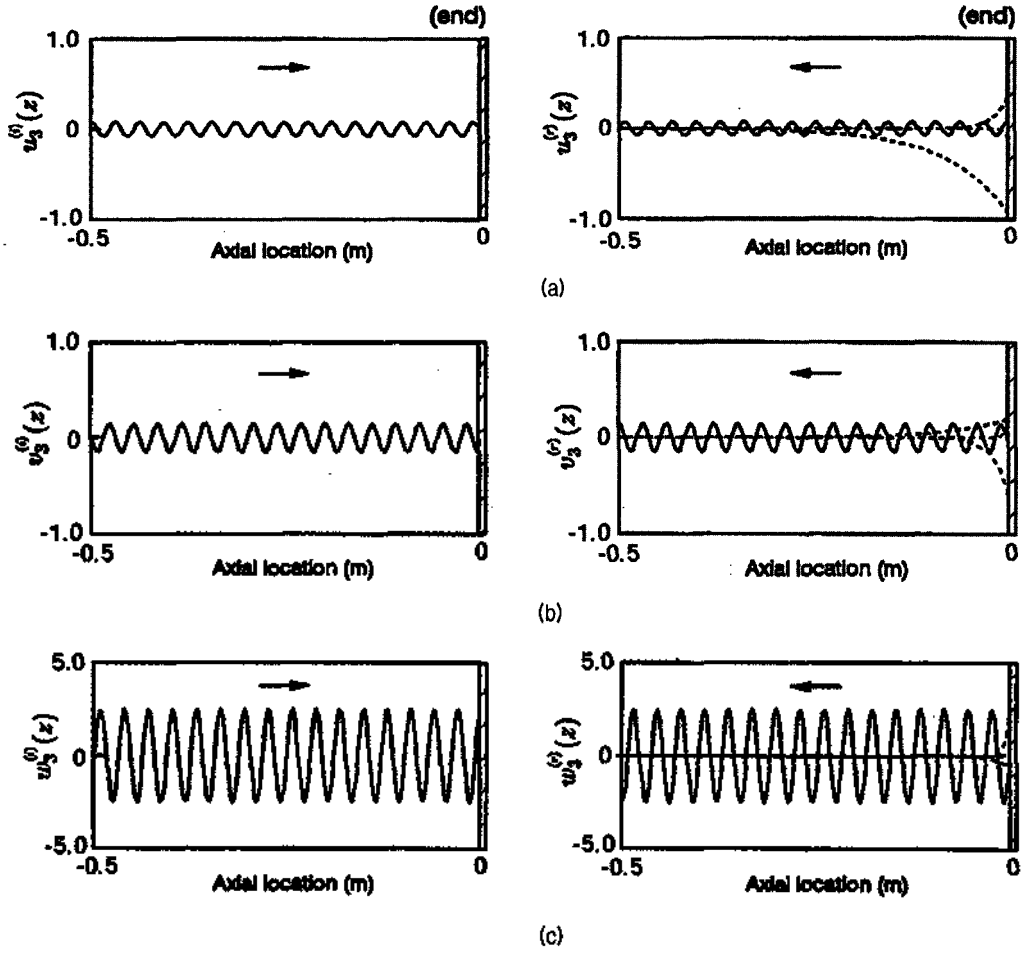


Figure 5. Mode conversion at the free end of the semi-infinite cylindrical shell (at $z=0$) at 18275 $Hz$ and $n=3$: waves exciting (a) the axial motion, (b) the circumferential motion and (c) the radial motion. ($\rightarrow$) and ($\leftarrow$) represent incident and reflected waves from the end of the shell, respectively. The curves (—) and (---) correspond to flexural waves and evanescent waves, respectively.

evanescent wave. The Prony decomposition of the data shows the presence of a wave number such that $k_z a = -0.11 + 0.92i$. This value is in good agreement with the theoretical value $k_z a = 0.98i$ calculated from the dispersion relation based on Donnell's shell equation[10].

The result in Fig. 4 shows that a strong evanescent wave field can be excited along about half the length of the shell. The evanescent wave generates the strong in-plane end vibration of the shell.

## III. Mode Conversion

In order to understand the phenomenon of the strong evanescent wave field at the end of the shell, the following analysis has been done. Consider a semi-infinite cylindrical shell with the same radius, thickness and material as the experimental model has. It has the free-free boundary condition at the end of the shell. The axial, circumferential and radial displacement components such ( $u_3(z)$ , $v_3(z)$ and $w_3(z)$ ) with the dependence of circumferential wave index $n=3$ are evaluated using the algorithm in Ref.[11]. The displacement field has been regarded as a superposition of propagating disturbances due to elastic waves, and the reflection of the waves at the end of the semi-infinite cylindrical shell has been considered.

At a frequency of 18275 $Hz$, flexural waves and evanescent waves are propagating with dependence of $n=3$ in the cylindrical shell, while flexural, longitudinal, shear and evanescent waves are propagating with the dependence of $n=1$. Consider the incident flexural and evanescent waves with dependence $n=3$ propagating from the source point to the end of the semi-infinite cylindrical shell. The location of the end of the shell is taken as $z=0$. Fig. 5 shows the incident flexural waves (denoted as $\rightarrow$) associated with axial, circumferential and radial displacement components ( $u_3(z)$ $v_3(z)$ and $w_3(z)$ ). It shows also that reflected waves (denoted as $\leftarrow$) are generated so that the boundary conditions at the end are satisfied in combination with the incident wave. The reflected waves include the evanescent waves as well as the propagating flexural waves. This phenomenon shows that the end of the shell as a structural discontinuity give rise to wavenumber conversion, or mode conversion. The strong evanescent wave is observed in the axial motion in Fig. 5 (a). This evanescent wave generates the strong in-plane vibration of the end of the shell. This result can be compared with the experimental result in Fig. 4.

The evanescent waves (with large imaginary wavenumber) in the experimental result in Fig. 4 are result of the mode conversion of the flexural waves into evanescent waves at the end of the shell. The evanescent waves are usually generated and localized to the region close to the structural discontinuities or the source point. However the results in Fig. 4 and Fig. 5 (a) show that a strong evanescent wave field can be excited along about half the length of the shell. It causes the strong in-plane end vibration of the shell.

## IV. Conclusions

In this paper, the strong in-plane vibration has been experimentally observed at the end of a cylindrical shell. It has been shown that the strong in-plane vibration has been generated due to the evanescent waves. It has been also shown that the evanescent waves are generated due to mode conversion of elastic waves at the ends of the cylindrical shells. The results show that the strong in-plane end vibration can be generated at ends of cylindrical shells. In this paper the strong end vibration with the circumferential mode $n=3$ has been observed at frequency 18275 $Hz$. More investigation is needed to see whether the end vibration with different circumferential modes can be generated at the ends of cylindrical shells at other frequencies.

## References

1. J. Oliver, "Elastic wave dispersion in a cylindrical rod by a wide-band short duration pulse technique," *J. Acoust. Soc. Am.* 29 (2), 189-194, 1957.

2. E. A. G. Shaw, "On the resonant vibrations of thick barium titanate disks," *J. Acoust. Soc. Am.*, **28** (1), 38-50, 1956.
3. D. C. Gazis, and R. D. Midlin, "Extensional vibrations and waves in a circular disk and a semi-infinite plates," *J. Appl. Mech.* 27, 541-547, 1960.
4. J. D. Kaplunov, L. Y. Kossovich, and M. V. Wilde, "Free localized vibrations of a semi-infinite cylindrical shell," *J. Acoust. Soc. Am.* **107** (3), 1383-1393, 2000.
5. H.-G. Kil, J. Jarzanski, and Y. H. Berthelot, "Wave decomposition of the vibrations of a cylindrical shell with automated scanning laser vibrometer," *J. Acoust. Am.* **104** (6), 3161-3168, 1998.
6. E. G. Williams, B. H. Houston, and J. A. Bucar, "Experimental Investigation of the wave propagation on a point-driven, submerged capped cylinder using k-space analysis," *J. Acoust. Am.* **87** (2), 513-522, 1990.
7. E. O. Brigham, The Fast Fourier Transform, Prentice-Hall, Inc., 1974.
8. S. L. Marple, Jr., Digital Spectral Analysis: with Application, Engle Cliffs, NJ, 1987, 303-304, 1987.
9. K. Grosh, and E. G. Williams, "Complex wave-number decomposition of structural vibrations," *J. Acoust. Am.* **93** (2), 836-838, 1993.
10. M. C. Junger and D. Feit, Sound, Structures, and Their Interactions, *Acoustical Society of America*, 216-218, 1993.
11. H.-G. Kil, "Wave interpretation of forced vibration of finite cylindrical shells," *J. Acoust. Soc. Korea*, **18** (2), 83-89, 1999.

## [Profile]

• Hyun-Gwon Kil

The Journal of the Acoustical Society of Korea Vol. 20, No. 4E, 2001.